Springer Link

Encyclopedia of Nanotechnology

2016 Edition
| Editors: Bharat Bhushan

Finite-Difference Frequency-Domain Technique

- Georgios Veronis (1) Email author (gveronis@lsu.edu)

1. Department of Electrical and Computer Engineering and Center for Computation and Technology, Louisiana State University, , Baton Rouge, USA

Reference work entry
First Online: 29 November 2016

DOI: https://doi.org/10.1007/978-94-017-9780-1_16

Definition

The finite-difference frequency-domain technique is a numerical technique for the solution of Maxwell's equations of electromagnetism in the frequency domain. It is based on approximating the derivatives in Maxwell's equations by finite differences, and results in a system of algebraic equations, which is solved using numerical linear algebra techniques.

Introduction to the Simulation of Plasmonic Devices

The finite-difference frequency-domain (FDFD) technique is a general-purpose numerical technique for the solution of Maxwell's equations of electromagnetism in the frequency domain. It can be applied to structures of any length scale and for sources of electromagnetic radiation of any frequency. Here, however, the focus is on the use of this technique in nano-optics, and in particular *plasmonics*.

Plasmonics is a rapidly evolving field of science and technology based on *surface plasmons*, which are electromagnetic waves that propagate along the interface of a metal and a dielectric. In surface plasmons, light interacts with the free electrons of the metal, which oscillate collectively in response to the applied field. Recently, nanometer scale metallic devices have shown the potential to manipulate light at the subwavelength scale using surface plasmons [1]. This could lead to photonic circuits of nanoscale dimensions.

Surface plasmons can be described by macroscopic electromagnetic theory, i.e., Maxwell's equations, if the electron mean free path in the metal is much shorter than the plasmon wavelength [2]. This condition is usually fulfilled at optical frequencies [2]. In macroscopic electromagnetic theory, bulk material properties, such as dielectric constant, are used to describe objects irrespective of their size. Here, all materials are assumed to be nonmagnetic $\left(\mu = \mu_0\right)$ and are characterized by their bulk dielectric constant $\epsilon(\mathbf{r}, \omega)$, where $\mathbf{r} = (x, y, z) = x\hat{x} + y\hat{y} + z\hat{z}$, and ω is the angular frequency. However, for particles of nanometer dimensions a more fundamental description of their optical and electronic properties may be required [3].

Analytical methods, such as Mie theory [4], can only be applied to planar geometries or to objects of specific shapes (spheres, cylinders) and have therefore limited importance in the analysis of plasmonic devices and structures. Numerical simulation techniques are therefore very important for the analysis and design of plasmonic devices. Numerical modeling of plasmonic devices involves several challenges which need to be addressed. First, as mentioned above, plasmonic devices can have arbitrary geometries. Several techniques are specific for one type of geometrical configuration and are therefore not appropriate for modeling of arbitrary plasmonic devices.

Second, the dielectric constant of metals at optical wavelengths is complex, i.e., $\varepsilon_r(\omega) = \varepsilon_{\mathrm{Re}}(\omega) + i\varepsilon_{\mathrm{Im}}(\omega)$ and is a complicated function of frequency [5]. Thus, several simulation techniques which are limited to lossless, nondispersive materials are not applicable to plasmonic devices. In addition, in time-domain methods the dispersion properties of metals have to be approximated by suitable analytical expressions [6]. In most cases, the *Drude model* is invoked to characterize the frequency dependence of the metallic dielectric function [7]

$$\varepsilon_{\mathrm{r,\,Drude}}(\omega) = 1 - \frac{\omega_p^2}{\omega(\omega + i\gamma)}, \tag{1}$$

where ω_p and γ are frequency-independent parameters. However, the Drude model approximation is valid over a limited wavelength range [7]. The range of validity of the Drude model can be extended by adding Lorentzian terms to Eq. 1 to obtain the *Lorentz-Drude model* [7]

$$\varepsilon_{r,\mathrm{LD}}(\omega) = \varepsilon_{r,\mathrm{Drude}}(\omega) + \sum_{j=1}^{k} \frac{f_j \omega_j^2}{\left(\omega_j^2 - \omega^2\right) - i\omega\gamma_j}, \tag{2}$$

where ω_j and γ_j stand for the oscillator resonant frequencies and bandwidths, respectively, and f_j are weighting factors. Physically, the Drude and Lorentzian terms are related to intraband (free electron) and interband (bound electron) transitions, respectively [7]. Even though the Lorentz-Drude model extends the range of validity of analytical approximations to metallic dielectric constants, it is not suitable for description of sharp absorption edges observed in some metals, unless a very large number of terms are used [7]. In particular, the Lorenz-Drude model cannot approximate well the onset of interband absorption in noble metals (Ag, Au, and Cu), even if five Lorentzian terms are used [7]. In Fig. 1, the Drude and Lorentz-Drude models are compared with experimental data for silver. It is observed that even a five-term Lorentz-Drude model with optimal parameters results in a factor of two error at certain frequencies.

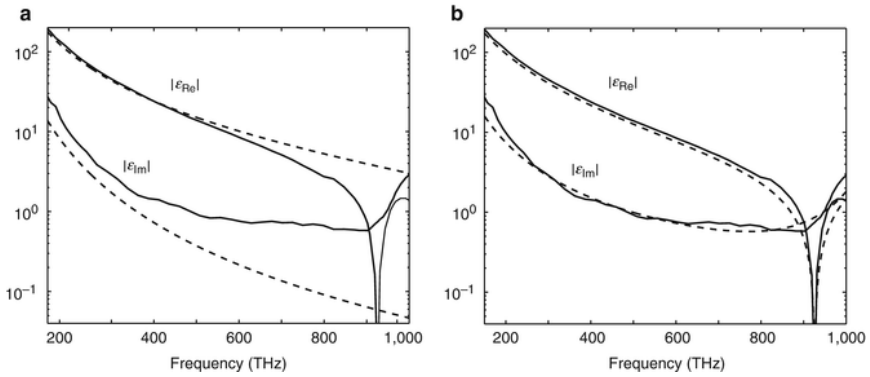

Finite-Difference Frequency-Domain Technique, Fig. 1

Real and imaginary part of the dielectric constant of silver at optical frequencies. The *solid lines* show experimental data [5]. The *dashed lines* show values calculated using (**a**) the Drude model and (**b**) the Lorentz-Drude model with five Lorentzian terms. The parameters of the models are optimal and obtained through an optimization procedure [7]

Third, in surface plasmons propagating along the interface of a metal and a dielectric, the field is concentrated at the interface and decays exponentially away from the interface in both the metal and dielectric regions [8]. Thus, for numerical methods based on discretization of the fields on a numerical grid, a very fine grid resolution is required at the metal-dielectric interface to adequately resolve the local fields. In addition, several plasmonic devices are based on components of subwavelength dimensions [8]. In fact, most of the potential applications of surface plasmons are related to subwavelength optics. The nanoscale feature sizes of plasmonic devices pose an extra challenge to numerical simulation techniques.

The challenges involved in modeling plasmonic devices will be illustrated here using a simple example: an infinite periodic array of silver cylinders illuminated by a plane wave at normal incidence (inset of Fig. 2a). The FDFD method, which is described in detail below, is used to calculate the transmission of the periodic array. This method allows one to directly use experimental data for the frequency-dependent dielectric constant of metals, including both the real and imaginary parts, with no approximation. The fields are discretized on a uniform two-dimensional (2-D) grid with grid size $\Delta x = \Delta y = \Delta l$. The calculated transmission as a function of frequency is shown in Fig. 2a. Also shown is the transmission of the structure calculated with the Drude model of Eq. 1. It is observed that the use of the Drude model results in substantial error. In general, the Drude model parameters are chosen to minimize the error in the dielectric function in a given frequency range [9]. However, this approach gives accurate results in a limited wavelength range, as illustrated in this example. In general, the complicated dispersion properties of metals at optical frequencies pose a challenge in modeling of plasmonic devices not encountered in modeling of low- or high-index-contrast dielectric devices.

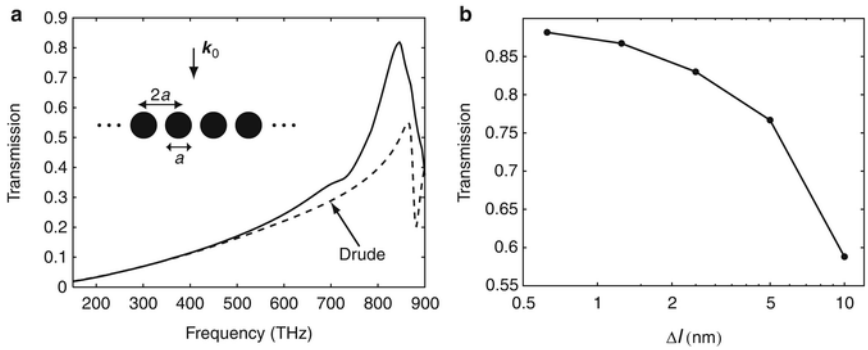

Finite-Difference Frequency-Domain Technique, Fig. 2

(**a**) Calculated transmission spectrum of an infinite array of silver cylinders (shown in the *inset*) for normal incidence and transverse magnetic (*TM*) polarization (involving only the E_x, E_y, and H_z vector field components). Results are shown for a diameter a = 100 nm. The *dashed line* shows the transmission spectrum calculated using the Drude model (Eq. 1) with parameters $\omega_p = 1.37 \times 10^{16} \mathrm{s}^{-1}$ and $\gamma = 7.29 \times 10^{13} \mathrm{s}^{-1}$. (**b**) Calculated transmission at 855 THz as a function of the spatial grid size Δl

The calculated transmission at a specific wavelength as a function of the spatial grid size Δl is shown in Fig. 2b. It is observed that a grid size of $\Delta l \cong 1$ nm is required in this case to yield reasonably accurate results. The required grid size is directly related to the decay length of the fields at the metal-dielectric interface. In general, modeling of plasmonic devices requires much finer gird resolution than modeling of low- or high-index-contrast dielectric devices, due to the high localization of the field at metal-dielectric interfaces of plasmonic devices. The required grid size depends on the shape and feature size of the modeled plasmonic device, the metallic material used, and the operating frequency.

In the following sections, the FDFD technique is introduced, and it is also examined how FDFD addresses the challenges mentioned above.

Introduction to Finite-Difference Methods

FDFD is based on approximating the derivatives in Maxwell's equations by finite differences. A brief overview of the main features of finite-difference methods is therefore first provided here. In finite-difference methods, derivatives in differential equations are approximated by finite differences. To approximate the derivative $df/dx|_{x_0}$ Taylor series expansions *f(x)* about the point x_0 at the point $x_0+\Delta x$ and $x_0-\Delta x$ are used to obtain [6]

$$\frac{df}{dx}\Big|_{x_0} = \frac{f(x_0+\Delta x) - f(x_0-\Delta x)}{2\Delta x} + O\left[(\Delta x)^2\right]. \quad (3)$$

Here, the notation $O[(\Delta x)^2]$ (to be read as " order$(\Delta x)^2$ ") denotes the remainder term and indicates its dependence on Δx, i.e., that it approaches zero as the second power of Δx. Thus, Eq. 3 shows that a *central-difference* approximation of the first derivative is *second-order accurate*, meaning that the remainder term in Eq. 3 approaches zero as the square of Δx.

In finite-difference methods, a continuous problem is approximated by a discrete one. Field quantities are defined on a discrete grid of nodes. The rectangular grid with node coordinates $\mathbf{r}_{ijk} = \left(x_i, y_j, z_k\right)$ is the simplest and most commonly used. A field quantity at nodal location $\mathbf{r}_{ijk}$ is denoted for convenience as $f|_{ijk} \equiv f\left(\mathbf{r}_{ijk}\right)$. Based on Eq. 3, the first derivative can be approximated by the following central-difference formula

$$\frac{df}{dx}\Big|_i \cong \frac{f|_{i+1} - f|_{i-1}}{2\Delta x},$$

(4)

which is second-order accurate, based on the discussion above, if the rectangular grid is uniform, i.e., $x_i = i\Delta x$. For example, if the numerical resolution in the x direction is increased by a factor of 10 ($\Delta x' = \Delta x/10$), then the error introduced by the finite-difference formula in Eq. 4 reduces roughly by a factor of $10^2 = 100$. Similarly, the second derivative can be approximated by the formula

$$\frac{d^2 f}{dx^2}\Big|_i \cong \frac{f|_{i+1} - 2f|_i + f|_{i-1}}{(\Delta x)^2},$$

(5)

which is also second-order accurate on a uniform grid [6].

By replacing derivatives in differential equations with their finite-difference approximations, algebraic equations are obtained, which relate the value of the field at a specific node to the values at neighboring nodes. By applying the finite-difference approximation to all nodes of the grid, a system of linear equations of the form $\mathbf{Ax} = \mathbf{b}$ is obtained. Since the equation for the field at each point involves only the fields at a few (typically two, four, and six in one, two, and three dimensions, respectively) adjacent points, the resulting system matrix is extremely sparse. Such problems can be solved efficiently if direct or iterative sparse matrix techniques are used.

The FDFD Method in One Dimension

The FDFD equations will now be derived by approximating the spatial derivatives in Maxwell's equations with finite differences. Assuming an exp($i\omega t$) harmonic time dependence for all field quantities, Maxwell's curl equations in the frequency domain take the form

$$\nabla \times \mathbf{E}(\mathbf{r}) = -i\omega\mu_0 \mathbf{H}(\mathbf{r}),$$

(6)

$$\nabla \times \mathbf{H}(\mathbf{r}) = \mathbf{J}(\mathbf{r}) + i\omega\varepsilon(\mathbf{r})\,\mathbf{E}(\mathbf{r}).$$

(7)

It should be noted that the field vectors $\mathbf{E}(\mathbf{r}, t)$, $\mathbf{H}(\mathbf{r}, t)$ are real (measurable) quantities that can vary with time, whereas the vectors $\mathbf{E}(\mathbf{r}, \omega)$, $\mathbf{H}(\mathbf{r}, \omega)$ are complex phasors that do not vary with time. The former can be obtained from the latter by multiplying by exp($i\omega t$) and taking the real part. For example,

$$\mathbf{E}(\mathbf{r}, t) = \mathrm{Re}\left\{\mathbf{E}(\mathbf{r}, \omega)\exp(i\omega t)\right\}.$$

(8)

It should also be noted that in most cases for simplicity the frequency dependence of the complex phasors is not explicitly shown, e.g., $\mathbf{E}(\mathbf{r})$ is used instead of $\mathbf{E}(\mathbf{r}, \omega)$. Maxwell's equations can be simplified by considering electromagnetic fields and systems with no variations in two dimensions, namely, both y and z. By dropping all

the y and z derivatives in Eqs. 6 and 7, and assuming a current source polarized in the z direction ($\mathbf{J} = J_z \hat{z}$), Maxwell's equations simplify to

$$\frac{\partial E_z}{\partial x} = i\omega\mu_0 H_y, \tag{9}$$

$$\frac{\partial H_y}{\partial x} = J_z + i\omega\varepsilon E_z. \tag{10}$$

In the *Finite-Difference Time-Domain* (FDTD) technique a staggered spatial grid, known as the *Yee grid* [6], is used for interleaved placement of the electric and magnetic fields. The Yee grid enables the approximation of the continuous derivatives in space by second-order-accurate two-point centered finite differences. Since the spatial derivatives involved in Maxwell's equations in the frequency domain are exactly the same as those in the time domain, the Yee grid can also be used in FDFD. The placement of the electric and magnetic fields on a one-dimensional (1-D) Yee grid for FDFD is identical to the one for FDTD and is shown in Fig. 3.

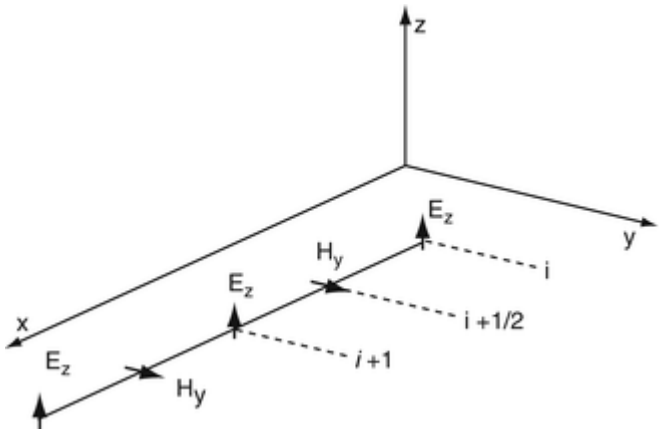

Finite-Difference Frequency-Domain Technique, Fig. 3

The placement of electric and magnetic field vectors in FDFD for Maxwell's equations in one dimension

For simplicity a uniform rectangular grid with $x_i = i\Delta x$ is considered, and the derivatives in Eqs. 9 and 10 are replaced with their finite-difference approximations to obtain

$$\frac{E_z|_{i+1} - E_z|_i}{\Delta x} = i\omega\mu_0 H_y|_{i+1/2}, \tag{11}$$

$$\frac{H_y|_{i+1/2} - H_y|_{i-1/2}}{\Delta x} = J_z|_i + i\omega\varepsilon|_i E_z|_i. \tag{12}$$

As mentioned above, by applying Eqs. 11 and 12 at all points in the Yee grid, a system of linear equations is obtained, which can be solved to find the electromagnetic fields. If the system obtained from Eqs. 11 and 12 was directly solved, all electric fields $\left(E_z|_1, E_z|_2, \ldots, E_z|_{N_x+1}\right)$ and all magnetic fields $\left(H_y|_{1+1/2}, H_y|_{2+1/2}, \ldots, H_y|_{N_x+1/2}\right)$ would have to be included in the vector of unknown fields. (A 1-D Yee grid terminated at electric field positions was assumed here.) Thus, the system of linear equations would have a total of $2N_x + 1$ unknowns. However, in the system of equations obtained from the FDFD algorithm, it is straightforward to eliminate either all the electric or all the magnetic fields. To see this, Eq. 11 is applied at two adjacent grid points:

$$\frac{1}{i\omega\mu_0}\frac{E_z|_i - E_z|_{i-1}}{\Delta x} = H_y|_{i-1/2},$$
(13)
$$\frac{1}{i\omega\mu_0}\frac{E_z|_{i+1} - E_z|_i}{\Delta x} = H_y|_{i+1/2}.$$
(14)
Equations 13 and 14 are now substituted into Eq. 12 to obtain
$$\frac{1}{\Delta x}\frac{1}{i\omega\mu_0}\left(\frac{E_z|_{i+1} - E_z|_i}{\Delta x} - \frac{E_z|_i - E_z|_{i-1}}{\Delta x}\right) = J_z|_i + i\omega\varepsilon|_i E_z|_i,$$
(15)
which can also be written as
$$\frac{1}{(\Delta x)^2}E_z|_{i-1} + \left[-\frac{2}{(\Delta x)^2} + \omega^2\varepsilon|_i\mu_0\right]E_z|_i$$

$$+\frac{1}{(\Delta x)^2}E_z|_{i+1} = i\omega\mu_0\, J_z|_i.$$
(16)
Thus, application of finite-difference approximations at the node location x_i results in a linear algebraic equation which relates the field $E_z|_i$ to the fields at the two adjacent nodes $E_z|_{i-1}$ and $E_z|_{i+1}$. By applying the finite-difference approximation to all internal nodes of the grid, a system of linear equations of the form $\mathbf{Ax} = \mathbf{b}$ is obtained, where $\mathbf{b}$ is determined by the source current $\mathbf{J}$:
$$a_{ii-1} = a_{ii+1} = \frac{1}{(\Delta x)^2},$$
$$a_{ii} = -\frac{2}{(\Delta x)^2} + \omega^2\,\varepsilon|_i\mu_0,$$
$$b_i = i\omega\mu_0\, J_z|_i,\ x_i = E_z|_i.$$
(17)
The FDFD equations for the boundary nodes depend on the boundary conditions at the boundary of the simulation domain. Typically, they involve only the two outermost nodes, e.g., $a_{11}x_1 + a_{12}x_2 = 0$. Thus, in the 1-D case the linear system matrix $\mathbf{A}$ is tridiagonal, and it is straightforward to eliminate the magnetic fields and obtain a system of equations which only involves the electric fields $\left(E_z|_1, E_z|_2, \ldots, E_z|_{N_x+1}\right)$ and has a total of $N_x + 1$ unknowns.

Finally, if Eqs. 9 and 10 are combined, the Helmholtz equation in 1-D is obtained:
$$\frac{\partial^2 E_z}{\partial x^2} + \omega^2\varepsilon\mu_0 E_z = i\omega\mu_0 J_z.$$
(18)
When the spatial derivatives in this equation are approximated by centered finite differences, Eq. 16 above is obtained. In other words, the FDFD equations can be directly obtained by discretizing the Helmholtz equation for the electric field.

The FDFD Method in Two and Three Dimensions

For the 2-D case, it is assumed that there are no variations of either the fields or the excitation in one of the directions, say the z direction. Thus, all derivatives with respect to z drop out from the two curl Eqs. 6 and 7. A current source polarized in the z direction ($\mathbf{J} = J_z\hat{z}$) is also assumed, so that only the transverse electric (TE)

polarization (involving only the $H_x, H_y,$ and E_z vector field components) is excited [6] and Maxwell's equations simplify to

$$\frac{\partial E_z}{\partial y} = -i\omega\mu_0 H_x,$$

$$\frac{\partial E_z}{\partial x} = i\omega\mu_0 H_y,$$

$$\frac{\partial H_y}{\partial x} - \frac{\partial H_x}{\partial y} = J_z + i\omega\varepsilon E_z.$$

(19)

If Eq. 19 are combined, the 2-D Helmholtz equation is obtained

$$\frac{\partial^2 E_z}{\partial x^2} + \frac{\partial^2 E_z}{\partial y^2} + \omega^2\varepsilon\mu_0 E_z = i\omega\mu_0 J_z.$$

(20)

As mentioned in the previous section, the exact same FDTD Yee grid can be used in FDFD. A portion of the Yee grid for the TE case is depicted in Fig. 4.

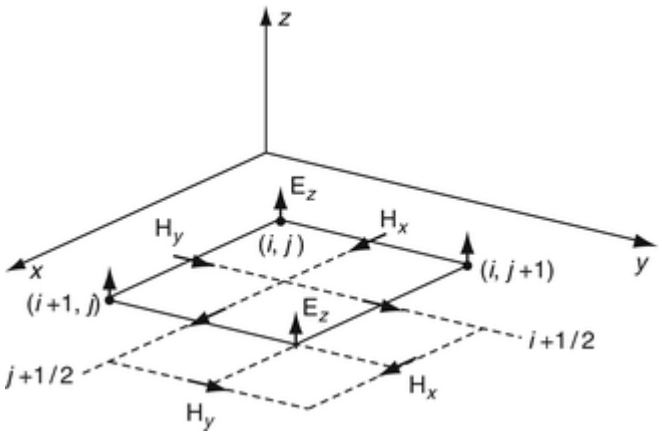

Finite-Difference Frequency-Domain Technique, Fig. 4

An FDFD unit cell for transverse electric (TE) waves. The small vectors with *thick arrows* are placed at the point in the grid at which they are defined. For example, E_z is defined at grid points (i, j), while H_y is defined at grid points $(i + 1/2, j)$

The FDFD equations can be obtained by discretizing (Eq. 19). It is then straightforward to eliminate H_x and H_y to obtain the FDFD equations which only involve the E_z field. Here, however, the 2-D Helmholtz equation (20) is discretized to directly obtain the FDFD equations which only involve the E_z field. Once E_z is calculated by solving the FDFD equations, the H_x and H_y fields can be calculated by using the discretized versions of Eq. 19.

For simplicity a uniform rectangular grid with $x_i = i\Delta x$ and $y_j = j\Delta y$ is considered, and the derivatives in Eq. 20 are replaced with their finite-difference approximations to obtain

$$\frac{E_z|_{i+1,j} - 2E_z|_{i,j} + E_z|_{i-1,j}}{(\Delta x)^2} + \frac{E_z|_{i,i+1} - 2E_z|_{i,i} + E_z|_{i,i-1}}{(\Delta y)^2} + \omega^2\varepsilon|_{i,j}\ \mu_0 E_z|_{i,j} = i\omega\mu_0 J_z|_{i,j}.$$

(21)

Thus, application of finite-difference approximations at the node location $\mathbf{r}_{ij} = \left(x_i, y_j\right)$ results in a linear algebraic equation which relates the field $E_z|_{i,j}$ to the

fields at the four adjacent nodes $E_z|_{i-1,j}$, $E_z|_{i+1,j}$, $E_z|_{i,j-1}$, $E_z|_{i,j+1}$. In the end, the finite-difference approximation is applied to all nodes of the grid to obtain one FDFD equation at each grid point (i, j). These equations form a system of linear equations $\mathbf{Ax} = \mathbf{b}$ with $(N_x + 1) \times \left(N_y + 1\right)$ equations and unknowns. The vector of unknown fields $\mathbf{x}$ will include the electric fields at all grid points (i, j), where $i = 1, 2, \ldots, N_x + 1 \text{and} j = 1, 2, \ldots, N_y + 1$. It should be noted that $\mathbf{x}$ is a 1-D vector. A one-to-one mapping between the 2-D electric field $E_z|_{i,j}, i = 1, 2, \ldots, N_x + 1, j = 1, 2, \ldots, N_y + 1$ and the 1-D vector of unknown fields $x_m, m = 1, 2, \ldots, (N_x + 1) \times \left(N_y + 1\right)$ should therefore be constructed. Choosing the right mapping is in general important and can affect the convergence of the system of linear equations. One simple mapping function in the 2-D case is $m\,(i, j) = (i - 1)\left(N_y + 1\right) + j.$

(22)

Using this one-to-one mapping function, the following system of linear equations is obtained:

$$\begin{aligned} a_{m(i,j)m(i-1,j)} &= a_{m(i,j)m(i+1,j)} = \frac{1}{(\Delta x)^2}, \\ a_{m(i,j)m(i,j-1)} &= a_{m(i,j)m(i,j+1)} = \frac{1}{(\Delta y)^2}, \\ a_{m(i,j)m(i,j)} &= -\frac{2}{(\Delta x)^2} - \frac{2}{(\Delta y)^2} + \omega^2 \varepsilon|_{i,j}\ \mu_0, \\ b_{m(i,j)} &= i\omega\mu_0\ J_z|_{i,j}, \\ x_{m(i,j)} &= E_z|_{i,j}. \end{aligned}$$

(23)

The same approach can be applied to obtain the FDFD equations for the 2-D TM polarization case, as well as for the three-dimensional (3-D) case.

Numerical Dispersion of the FDFD Algorithm

A single plane wave propagating in a uniform medium has a simple *dispersion relation* connecting the angular frequency ω and the wave number k : $\omega = ck$ [10], where c is the speed of light in the medium. Numerical techniques such as the FDFD technique introduce *numerical dispersion*. To derive the dispersion properties of the FDFD algorithm, a single wave or Fourier mode in space is considered. The dispersive properties of FDFD are assessed by obtaining the dispersion relation of the scheme, relating the frequency of a Fourier mode on the grid to a particular wavelength λ (or wave number k):

$\omega = f_{\text{FDFD}}\,(k, \Delta x)\,.$

(24)

In the 1-D case, a plane wave propagating in a uniform medium is considered

$E(x) = e^{\sqrt{-1}kx},$

(25)

and its discretized version is

$E|_i = e^{\sqrt{-1}ki\Delta x}.$

(26)

In the above equations, $\sqrt{-1}$ was used to avoid confusing it with the grid index i. In a uniform medium with no sources the FDFD equation (16) becomes

$$\frac{E_z|_{i+1} - 2E_z|_i + E_z|_{i-1}}{(\Delta x)^2} + \omega^2 \varepsilon\mu_0\ E_z|_i = 0.$$

(27)

Equation 26 is substituted into Eq. 27 to find

$$\frac{e^{\sqrt{-1}ki\Delta x}\left(e^{\sqrt{-1}k\Delta x}-2+e^{-\sqrt{-1}k\Delta x}\right)}{(\Delta x)^2}+\omega^2\varepsilon\mu_0 e^{\sqrt{-1}ki\Delta x}=0,$$

(28)

from which one obtains

$$\omega = ck\left(\frac{\sin\left(\frac{k\Delta x}{2}\right)}{\frac{k\Delta x}{2}}\right).$$

(29)

Equation 29 is the dispersion relation of 1-D FDFD. It is observed that, in the limit $\Delta x \to 0$, Eq. 29 reduces to the exact dispersion relation $\omega = ck$. Using Eq. 29, the numerical phase velocity $\bar{v}_p \equiv \frac{\omega}{k}$ and group velocity $\bar{v}_g \equiv \frac{\partial\omega}{\partial k}$ of the FDFD scheme can be derived. The numerical phase velocity of 1-D FDFD as a function of the numerical resolution $\Delta x/\lambda$ is shown in Fig. 5. It is observed, for example, that for a spatial resolution of 20 grid points per wavelength ($\Delta x/\lambda = 0.05$) the numerical error in the phase velocity is less than 1 %.

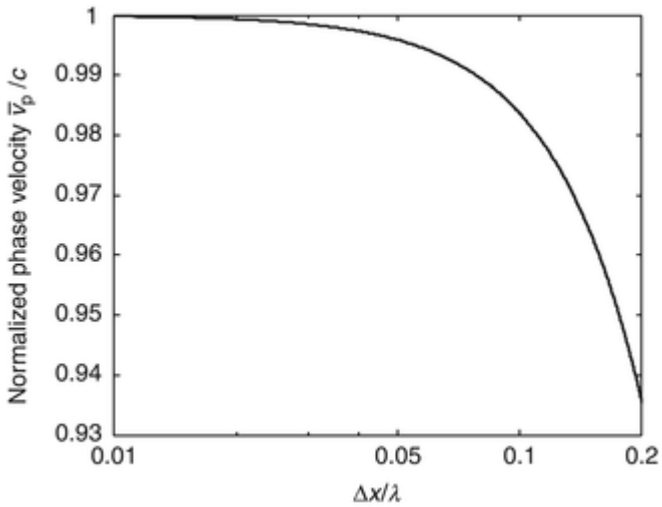

Finite-Difference Frequency-Domain Technique, Fig. 5

Dispersion of 1-D FDFD. Variation of numerical phase velocity with numerical resolution $\Delta x/\lambda$ in 1-D FDFD

In the 2-D case, wave-like modes propagating in both x and y directions are considered

$$E(x, y) = e^{\sqrt{-1}(k_x x + k_y y)},$$

(30)

and their discretized version is

$$E|_{i,j} = e^{\sqrt{-1}(k_x i\Delta x + k_y j\Delta y)},$$

(31)

where k_x and k_y are the wave numbers in the x and y directions, respectively.

In a uniform medium with no sources, the 2-D FDFD equation (21) becomes

$$\frac{E_z|_{i+1,j}-2E_z|_{i,j}}{(\Delta x)^2}+\frac{E_z|_{i,j+1}-2E_z|_{i,j}+E_z|_{i,j-1}}{(\Delta y)^2}+\omega^2\varepsilon\mu_0\, E_z|_{i,j}=0.$$

(32)

Equation 31 is substituted into Eq. 32 to find after some manipulation:

$$\omega^2 = c^2 \left[k_x^2 \left(\frac{\sin\left(\frac{k_x \Delta x}{2}\right)}{\frac{k_x \Delta x}{2}} \right)^2 + k_y^2 \left[\frac{\sin\left(\frac{k_y \Delta y}{2}\right)}{\frac{k_y \Delta y}{2}} \right]^2 \right].$$

(33)

It is observed again that, in the limit $\Delta x \to 0$ and $\Delta y \to 0$, Eq. 33 reduces to the exact dispersion relation $\omega^2 = c^2 \left(k_x^2 + k_y^2\right)$.

It can be seen from Eq. 33 that the numerical phase velocity $\bar{v}_p$ for the 2-D case is a function of angle of propagation through the FDFD grid. To see this, wave propagation at an angle θ with respect to the positive x axis is assumed, in which case $k_x = k \cos\theta$ and $k_y = k \sin\theta$, where $k = \sqrt{k_x^2 + k_y^2}$ is the wave number. Figure 6 shows a plot of normalized numerical phase velocity as a function of propagation angle θ. The dependence is, in general, relatively small (compared to dispersion errors due to the discretized grid), with $\bar{v}_p/c$ varying by only a few percent between θ = 45° and θ = 0°, even for very coarse (e.g., $\Delta x = \Delta y = \lambda_0/5$) spatial grids. The dependence of $\bar{v}_p$ on propagation angle θ is known as *grid anisotropy* and is a source of additional numerical dispersion effects.

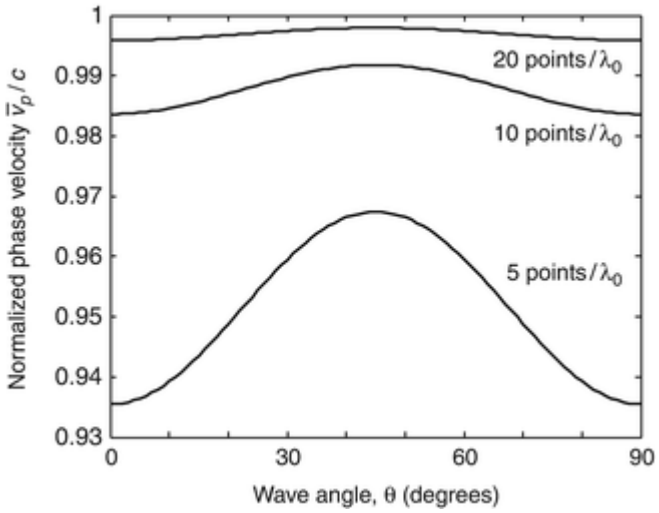

Finite-Difference Frequency-Domain Technique, Fig. 6

Dispersion of 2-D FDFD. Variation of numerical phase velocity with wave-propagation angle in a 2-D FDFD grid for three different cases of numerical resolution

Finally, it is noted that, unlike FDTD, in FDFD only the spatial derivatives are approximated by finite differences. In fact, for time-harmonic sources and fields the FDTD equations reduce to the FDFD equations in the limit of $\Delta t \to 0$.

Waveguiding Structures

In the previous sections, it was described how Maxwell's equations are solved with the FDFD method when the fields are excited by a current source **J**. A slightly different approach is required if one is interested in determining the modes and the dispersion characteristics of waveguiding structures which are uniform in the z direction. If all

field components have an $\exp(-\gamma z)$ dependence, it can be shown that Maxwell's equations reduce to [11]

$$-\varepsilon_r k_0^2 h_x + \varepsilon_r \frac{\partial}{\partial y}\left[\varepsilon_r^{-1}\left(\frac{\partial h_y}{\partial x} - \frac{\partial h_x}{\partial y}\right)\right]$$

$$-\frac{\partial}{\partial x}\left(\frac{\partial h_x}{\partial x} + \frac{\partial h_y}{\partial y}\right) = \gamma^2 h_x,$$

(34)

$$-\varepsilon_r k_0^2 h_y - \varepsilon_r \frac{\partial}{\partial x}\left[\varepsilon_r^{-1}\left(\frac{\partial h_y}{\partial x} - \frac{\partial h_x}{\partial y}\right)\right]$$

$$-\frac{\partial}{\partial y}\left(\frac{\partial h_x}{\partial x} + \frac{\partial h_y}{\partial y}\right) = \gamma^2 h_y,$$

(35)

where $\mathbf{H}(x, y, z) = \mathbf{h}(x, y)\exp(-\gamma z)$. Equations 34 and 35 also satisfy the transversality constraint for the magnetic field ($\nabla \cdot \mathbf{H} = 0$). They are discretized by applying the finite-difference method on the Yee grid. A sparse matrix eigenvalue problem of the form $\mathbf{Ah} = \gamma^2 \mathbf{h}$ is then obtained, which can be solved using iterative sparse eigenvalue techniques [12]. An important feature of this formulation is the absence of spurious modes in the solution [12], which is therefore robust.

Quasistatic Approximation

Several plasmonic structures have dimensions much smaller than the wavelength λ of the incident light. Under these conditions, retardation effects are negligible and the quasistatic approximation $\mathbf{E}(\mathbf{r}) = -\nabla\varphi(\mathbf{r})$ can be used for the scattered electric field, where $\varphi(\mathbf{r})$ is the electrostatic potential. The field distribution problem then reduces to solving [13]

$$\nabla \cdot \left\{\varepsilon(\mathbf{r})\left[-\nabla\varphi(\mathbf{r}) + \mathbf{E}^i(\mathbf{r})\right]\right\} = 0,$$

(36)

which represents the current conservation law. Equation 36 is discretized using the finite-difference method, as described above. A sparse system of linear equations of the form $\mathbf{Ax} = \mathbf{b}$ is obtained, where $\mathbf{b}$ is determined by the incident field $\mathbf{E}^i(\mathbf{r})$.

Comparison to Other Numerical Techniques

FDFD is a frequency-domain technique and can thus treat arbitrary material dispersion. Nonuniform and/or nonorthogonal grids are required in FDFD for efficient treatment of curved surfaces and rapid field variations at material interfaces. In FDFD, as in all other methods which are based on discretization of the differential form of Maxwell's equations in a finite volume, absorbing boundary conditions (ABCs) are required, so that waves are not artificially reflected at the boundaries of the computational domain. Very efficient and accurate ABCs, such as the perfectly matched layer (PML) [6, 12], have been demonstrated for FDFD. As mentioned above, FDFD results in extremely sparse systems of linear equations. Such problems can be solved efficiently if direct or iterative sparse matrix techniques are used.

FDTD is also a finite-difference method, so its performance in modeling plasmonic devices is similar to the performance of FDFD. There are many similarities between the two techniques. Both can be used to model structures with arbitrary geometries. In addition, many of the methods used in combination with FDTD (total field/scattered field method, etc.) can also be used with FDFD. However, there are some major differences. First, as already mentioned above, in time-domain methods the dispersion properties of metals have to be approximated by suitable analytical expressions which introduce substantial error in broadband calculations. In addition, the implementation of methods for dispersive materials in FDTD requires additional computational cost and extra memory storage [6, 14]. On the other hand, in FDTD it is possible to obtain the entire frequency response with a single simulation by exciting a broadband pulse and calculating the Fourier transform of both the excitation and the response [6].

The *Finite-Element Frequency-Domain* (FEFD) method is a more powerful technique than FDFD, especially for problems with complex geometries. However, FDFD is conceptually simpler and easier to program. The main advantage of FEFD is that complex geometric structures can be discretized using a variety of elements of different shapes, while in FDFD a rectangular grid is typically used leading to staircase approximations of particle shapes [12, 15]. In addition, in FEFD fields within elements are approximated by shape functions, typically polynomials, while in FDFD a simpler piecewise constant approximation is used [15]. In short, FEFD is more complicated than FDFD but achieves better accuracy for a given computational cost [15].

Future Research Directions

The dispersion properties of metals at optical frequencies are a major challenge in modeling of plasmonic devices. Frequency-domain techniques can treat arbitrary material dispersion but require a large number of simulations to obtain the broadband response. One possible future research direction could be the development of suitable fast frequency-sweep methods [12]. Such methods allow the computation of the broadband response by simulating the device only at a limited number of frequencies. Another major challenge in modeling of plasmonic devices is the very fine discretization required to adequately resolve the rapid field decay away from metal-dielectric interfaces. Although nonuniform and/or nonorthogonal grids increase the efficiency of standard numerical methods for such problems, it would be interesting to investigate whether numerical grids could be optimized specifically for treatment of plasmonic devices. Finally, the development of efficient numerical linear algebra techniques for the solution of the sparse systems of algebraic equations resulting from FDFD is also a major challenge. While there are general-purpose iterative techniques and preconditioners, it would be interesting to investigate whether such numerical linear algebra tools could be fine-tuned for frequency-domain simulation of plasmonic devices. In conclusion, there are many exciting research opportunities in developing more accurate and more efficient methods for plasmonic devices.

Cross-References

- Finite Element Methods for Computational Nano-optics (https://doi.org/10.1007/978-94-017-9780-1_17)

- Finite-Difference Time-Domain Technique (https://doi.org/10.1007/978-94-017-9780-1_15)

References

1. Maier, S.A.: Plasmonics: Fundamentals and Applications. Springer, New York (2007)
   Google Scholar (http://scholar.google.com/scholar_lookup?title=Plasmonics%3A%20Fundamentals%20and%20Applications&author=SA.%20Maier&publication_year=2007)
2. Novotny, L., Hecht, B., Pohl, D.W.: Interference of locally excited surface plasmons. J. Appl. Phys. **81**, 1798–1806 (1997)
   CrossRef (https://doi.org/10.1063/1.364036)
   Google Scholar (http://scholar.google.com/scholar_lookup?title=Interference%20of%20locally%20excited%20surface%20plasmons&author=L.%20Novotny&author=B.%20Hecht&author=DW.%20Pohl&journal=J.%20Appl.%20Phys.&volume=81&pages=1798-1806&publication_year=1997)
3. Prodan, E., Nordlander, P., Halas, N.J.: Effects of dielectric screening on the optical properties of metallic nanoshells. Chem. Phys. Lett. **368**, 94–101 (2003)
   CrossRef (https://doi.org/10.1016/S0009-2614(02)01828-6)
   Google Scholar (http://scholar.google.com/scholar_lookup?title=Effects%20of%20dielectric%20screening%20on%20the%20optical%20properties%20of%20metallic%20nanoshells&author=E.%20Prodan&author=P.%20Nordlander&author=NJ.%20Halas&journal=Chem.%20Phys.%20Lett.&volume=368&pages=94-101&publication_year=2003)
4. Bohren, C.F., Huffman, D.R.: Absorption and Scattering of Light by Small Particles. Wiley, New York (1983)
   Google Scholar (http://scholar.google.com/scholar_lookup?title=Absorption%20and%20Scattering%20of%20Light%20by%20Small%20Particles&author=CF.%20Bohren&author=DR.%20Huffman&publication_year=1983)
5. Palik, E.D. (ed.): Handbook of Optical Constants of Solids. Academic, New York (1985)
   Google Scholar (http://scholar.google.com/scholar_lookup?title=Handbook%20of%20Optical%20Constants%20of%20Solids&publication_year=1985)
6. Taflove, A.: Computational Electrodynamics. Artech House, Boston (1995)
   Google Scholar (http://scholar.google.com/scholar_lookup?title=Computational%20Electrodynamics&author=A.%20Taflove&publication_year=1995)
7. Rakic, A.D., Djurisic, A.B.., Elazar, J.M., Majewski, M.L.: Optical properties of metallic films for vertical cavity optoelectronic devices. Appl. Opt. **37**, 5271–5283 (1998)
   CrossRef (https://doi.org/10.1364/AO.37.005271)
   Google Scholar (http://scholar.google.com/scholar_lookup?title=Optical%20properties%20of%20metallic%20films%20for%20vertical%20

cavity%20optoelectronic%20devices&author=AD.%20Rakic&author=AB.%20Djurisic&author=JM.%20Elazar&author=ML.%20Majewski&journal=Appl.%20Opt.&volume=37&pages=5271-5283&publication_year=1998)

8. Barnes, W.L., Dereux, A., Ebbesen, T.W.: Surface plasmon subwavelength optics. Nature **424**, 824–830 (2003)
CrossRef (https://doi.org/10.1038/nature01937)
Google Scholar (http://scholar.google.com/scholar_lookup?title=Surface%20plasmon%20subwavelength%20optics&author=WL.%20Barnes&author=A.%20Dereux&author=TW.%20Ebbesen&journal=Nature&volume=424&pages=824-830&publication_year=2003)

9. Vial, A., Grimault, A.S., Macias, D., Barchiesi, D., De la Chapelle, M.L.: Improved analytical fit of gold dispersion: application to the modeling of extinction spectra with a finite-difference time-domain method. Phys. Rev. B **71**, 85416 (2005)
CrossRef (https://doi.org/10.1103/PhysRevB.71.085416)
Google Scholar (http://scholar.google.com/scholar_lookup?title=Improved%20analytical%20fit%20of%20gold%20dispersion%3A%20application%20to%20the%20modeling%20of%20extinction%20spectra%20with%20a%20finite-difference%20time-domain%20method&author=A.%20Vial&author=AS.%20Grimault&author=D.%20Macias&author=D.%20Barchiesi&author=ML.%20Chapelle&journal=Phys.%20Rev.%20B&volume=71&pages=85416&publication_year=2005)

10. Jackson, J.D.: Classical Electrodynamics. Wiley, New York (1999)
Google Scholar (http://scholar.google.com/scholar_lookup?title=Classical%20Electrodynamics&author=JD.%20Jackson&publication_year=1999)

11. Pereda, J.A., Vegas, A., Prieto, A.: An improved compact 2D fullwave FDFD method for general guided wave structures. Microw. Opt. Technol. Lett. **38**, 331–335 (2003)
CrossRef (https://doi.org/10.1002/mop.11052)
Google Scholar (http://scholar.google.com/scholar_lookup?title=An%20improved%20compact%202D%20fullwave%20FDFD%20method%20for%20general%20guided%20wave%20structures&author=JA.%20Pereda&author=A.%20Vegas&author=A.%20Prieto&journal=Microw.%20Opt.%20Technol.%20Lett.&volume=38&pages=331-335&publication_year=2003)

12. Jin, J.: The Finite Element Method in Electromagnetics. Wiley, New York (2002)
Google Scholar (http://scholar.google.com/scholar_lookup?title=The%20Finite%20Element%20Method%20in%20Electromagnetics&author=J.%20Jin&publication_year=2002)

13. Genov, D.A., Sarychev, A.K., Shalaev, V.M.: Plasmon localization and local field distribution in metal-dielectric films. Phys. Rev. E **67**, 56611 (2003)
CrossRef (https://doi.org/10.1103/PhysRevE.67.056611)
Google Scholar (http://scholar.google.com/scholar_lookup?title=Plasmon%20localization%20and%20local%20field%20distribution%20in%20metal-dielectric%20films&author=DA.%20Genov&author=AK.%20Sarychev&author=VM.%20Shalaev&journal=Phys.%20Rev.%20E&volume=67&pages=56611&publication_year=2003)

14. Young, J.L., Nelson, R.O.: A summary and systematic analysis of FDTD algorithms for linearly dispersive media. IEEE Antennas Propag. Mag. **43**, 61–

77 (2001)
CrossRef (https://doi.org/10.1109/74.920019)
Google Scholar (http://scholar.google.com/scholar_lookup?title=A%20summary%20and%20systematic%20analysis%20of%20FDTD%20algorithms%20for%20linearly%20dispersive%20media&author=JL.%20Young&author=RO.%20Nelson&journal=IEEE%20Antennas%20Propag.%20Mag.&volume=43&pages=61-77&publication_year=2001)

15. Sadiku, M.N.O.: Numerical Techniques in Electromagnetics. CRC Press, Boca Raton (2001)
Google Scholar (http://scholar.google.com/scholar_lookup?title=Numerical%20Techniques%20in%20Electromagnetics&author=MNO.%20Sadiku&publication_year=2001)

Copyright information

How to cite

Cite this entry as:

Veronis G. (2016) Finite-Difference Frequency-Domain Technique. In: Bhushan B. (eds) Encyclopedia of Nanotechnology. Springer, Dordrecht. https://doi.org/10.1007/978-94-017-9780-1_16

About this entry

- First Online 29 November 2016
- DOI https://doi.org/10.1007/978-94-017-9780-1
- Publisher Name Springer, Dordrecht
- Print ISBN 978-94-017-9779-5
- Online ISBN 978-94-017-9780-1
- eBook Packages Chemistry and Materials Science Reference Module Physical and Materials Science